

Original Article

# A Coiling-Up Metamaterial for Acoustic Band-Stop Filtering

Seonggeon Bae

School of ICT Convergence Engineering, Kangnam University, Youngin-si, Gyungg,y Korea.

Corresponding Author : [sgbae@kangnam.ac.k](mailto:sgbae@kangnam.ac.k)

Received: 13 November 2024

Revised: 16 April 2025

Accepted: 05 May 2025

Published: 31 May 2025

**Abstract** - In this study uses the efficient refractive index and efficient impedance to analyze two coiling-up structures with differing sound pressure. These structures have a high effective refractive index and effective impedance. To calculate the resonance frequencies, the coiling structures were modelled as a simple medium<sup>7, 8, 13</sup>. Our study calculated the sound pressure using the Fabry-Perot resonance theory. The application of this calculation applies to the different features of both open and closed cavity structures. In other words, it acts as a band-stop filter to reduce specified frequencies. We designed a metamaterial as an acoustic filter to attenuate or reject the desired frequency components using two types of cavities. Sound pressure typically appears as a periodic feature in the open cavity structure. In the closed cavity structure, the sound pressure produces attenuation due to the effects of the reflections on the slab. At the end of the transmission, the characteristics of the FP are maintained and the specified frequency components exhibit attenuation. These features can be applied to acoustic focusing, cloaking and filtering.

**Keywords** - Coiling-up, Sound pressure, Open and closed cavity, Fabry-Perot resonance, Metamaterial.

## 1. Introduction

To deform acoustic energy in a small volume, it is essential to create both a high impedance and high refraction index using an efficient acoustic structure that employs a coiling up of the structure. Naturally occurring materials with both a high impedance and high refractive index are rare, as an increase in density in materials is due to an increase in the velocity of sound pressure. Generally, acoustic attenuation parameters such as air, water, and metal are proportional to the frequency squared.

This means that there is a high loss in high frequencies. Attenuation rates are high at high frequencies and low at low frequencies. Low-frequency signals are used for underwater sound, and low-frequency signals are used for underwater acoustic communication over hundreds of kilometers. High frequencies are used for Ultrasound imaging.

As such, studies of acoustic metamaterials have been proceeding in order to find ways to control the propagation of sound waves. Acoustic metamaterials can be made through an approximate analysis of the effective refraction factor,  $n$  and the effective impedance,  $Z$ , of the artificial structures. Studies of many acoustic metamaterials are largely carried out to modify the propagation characteristics of sound waves. Metamaterials can be analyzed by calculating their effective refraction index and their effective impedance in an artificial structure.

## 2. Existing Method

To solve the transmission and reflection coefficients of our cavity, Fabry-Perot theory and acoustic numerical retrieval scattering methods 28 32 are used. The transmission coefficient,  $T$ , the reflection coefficient, and  $R$  of the metamaterial can be calculated using the effective medium parameter from the incident, as well as reflective and transmission waves. Assuming the amplitude of the displacement of the incident wave as 1, the reflective wave as  $R$  and the transmission wave as  $T$ , the amplitude of displacements,  $P(x, z)$ , on the slab as  $A$  and  $B$  are expressed as Equation 1.

$$P(x, z) = \begin{cases} e^{ik_z z} (e^{ik_x x} + R e^{-ik_x x}), & x < 0 \\ e^{ik_z z} (A e^{ik_x x} + B e^{-ik_x x}), & 0 < x < L \quad (1) \\ T e^{-ik_z z} e^{ik_x (x-L)}, & x < L \end{cases}$$

Where is the radial frequency,  $k$ , the wave number, is,  $A$  is the amplitude of the forward propagating wave, and  $B$  is the amplitude of the backward propagating wave, and the frequency of our cavity structures, which consists of a volume cavity with open and closed coiling up is calculated by equation 1. Figure 1 demonstrates the amplitude of displacements of our metamaterial cavity. In calculating, the pressure field and normal velocities are considered by continuity at  $x=0$  and  $x=L$  on the slab. By applying density and acoustic speed  $c$ , the transmission and reflection



coefficient for incident waves on the slab with density and acoustic velocity are considered as density and the acoustic velocity of air.

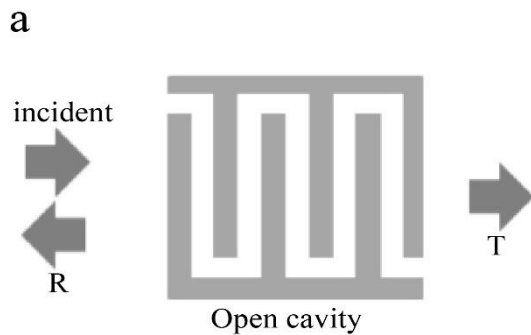
$$T = \frac{4Z_1Z_2}{(Z_1 - Z_2)(Z_2 - Z_1)e^{i\phi} + (Z_1 + Z_2)^2} \quad (2)$$

$$R = \frac{(Z_1 + Z_2)(Z_2 - Z_1)e^{-2i\phi} + (Z_1 - Z_2)(Z_1 + Z_2)}{(Z_1 + Z_2)(Z_2 - Z_1)e^{-2i\phi} - (Z_1 - Z_2)^2} \quad (3)$$

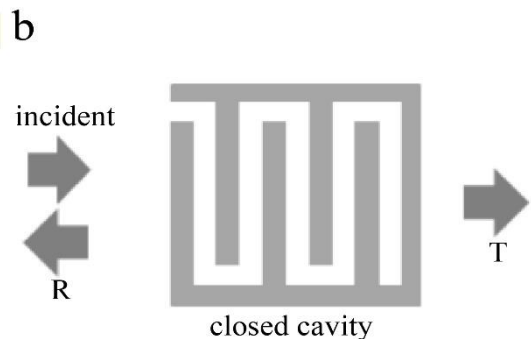
Where  $Z$  is the impedance,  $\phi$  is the angle between the incident wave and the slab,  $\phi$  is the phase,  $f$  is the frequency of the incident wave, and  $L$  is the slab thickness. In the loss of transmission condition, the reflection and transmission index ratio is determined by the density by  $\rho$ , Young's modulus by  $E$ , the shear modulus by  $G$ , and Poisson's ratio by  $\nu$ . To reduce the loss of transmission, the material with a small Poisson ratio is applied. Also, to satisfy,  $T = 1$  is considered in the full transmission. The effective refractive index  $n$  and effective impedance  $Z$  are obtained from the complex reflection and transmission coefficients for a plane wave normally incident on the slab. The effective density and speed of sound is calculated as follows: 2, 3

$$n = \frac{\pm \cos^{-1}\left(\frac{(1-R^2+T^2)}{2T}\right)}{kd} \quad (4)$$

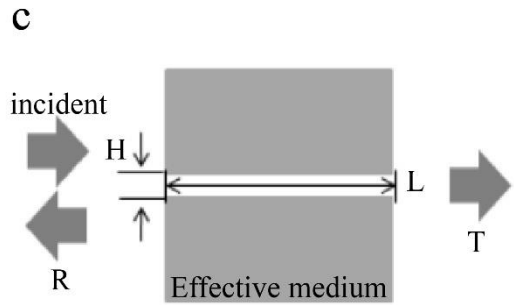
Where  $k$  is the wave number and  $d$  is the unit cell dimension.



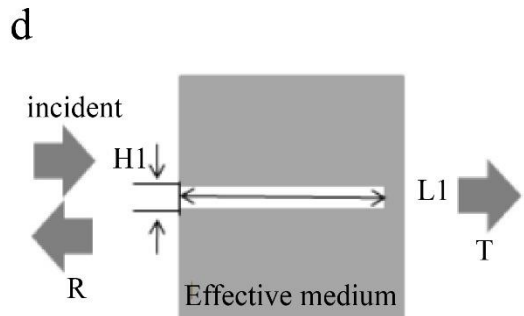
(a) A coiling-up structure in an open cavity used to produce identical path lengths of  $L$  and width  $w$



(b) A coiling-up structure in a closed cavity used to produce identical path lengths of  $L$  and width  $w$



(c) The effective medium of the open cavity structure shown in (a) using the refractive index and impedance



(d) The effective medium of the closed cavity structure is shown in (b) using the refractive index and impedance

Fig. 1 Transmission and reflection coefficients of two coiling up structures

The sound pressure for transmission changes in the slab depends on these coefficients and is inversely proportional to wave path lengths  $L$ ,  $L_c$  and heights  $H$ ,  $H_c$ . Therefore, it is possible to shift the amplitude of transmission to higher frequencies by increasing  $L$  and control frequency bandwidth by increasing  $H$  in the open cavity and, further, to attenuate the amplitude of reflection lower by increasing  $L_c$  and the control frequency bandwidth by increasing  $H_c$  in the closed cavity in calculation. After using FP resonance, the gain and bandwidth in the desired frequency can be controlled [1][2][3][5][11].

### 3. Proposed Method

Recent analyses of acoustic characteristics mainly use the Fabry-Perot theory as opposed to the classic Helmholtz resonant analysis. This can achieve satisfactory results at a very small scale to achieve the effective coefficients through an analysis of the characteristics of the incident and the reflected waves by using the effective refractive index and impedance. Thus, as shown in Figure 2, we can model the coiling up structures to two effective mediums.

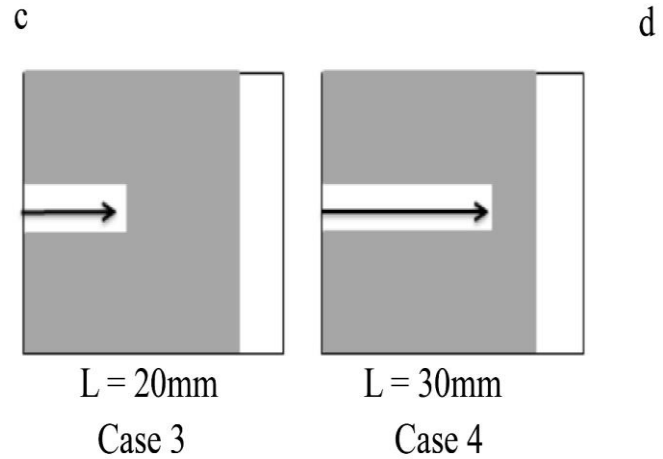
By using both an open and closed cavity, the transmission coefficients and the reflection coefficients can be obtained, as shown in Figures 2(b) and (d). Figures 2(a) (b) show the change in the transmission coefficient according to the length of the cavity in this structure of variable depth ( $L$ ). Figure 2

(b) shows a frequency-dependent reflection coefficient that corresponds to the width ( $w$ ) and depth ( $L$ ) of the cavity. The FP resonance frequency is calculated in the coiling-up structure, and the respective effective refractive indexes are  $n = 2.23$  and  $n = 3.16$  in the flange width  $w = 10\text{mm}$ , lengths  $L = 40\text{mm}$  and  $60\text{mm}$ .

As shown in Figure 2 (d), when the reflection coefficient is 4.12 in  $L = 80\text{mm}$  and 6.08 in  $120\text{mm}$ , this effect, with an increasing coefficient, will be a lower stop-band frequency. This study uses an open and closed coiling-up cavity. The open cavity has Fabry-Perot resonance characteristics, and the closed cavity has stop-band characteristics due to the refractive index.

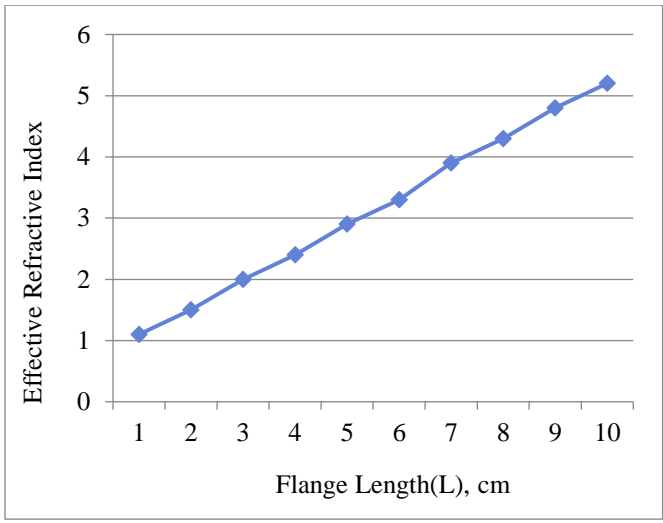
These sound pressure changes can be obtained by using transmission coefficients and reflection coefficients. As shown in Figures 3(a) and (c), the effective refractive index and the effective impedance are proportional to the size of the flange; that is, the change of sound pressure is proportional to the length of the flange. This appears differently depending on the length  $a$ , width  $w$  and depth  $d$  of the unit cells. As shown in Figure 3(b), in the flange, the effective refractive index is inversely proportional to the width  $w$  and depth  $d$ .

This is applicable when making highly effective refractive index metamaterial. Figure 3(d) compares the flange length changes for the two coiling up structures and shows the maximum FP resonance frequency and the minimum FP resonance frequency in transmission and reflection. The dimension of the flange used in the simulation was  $d = 1\text{ mm}$  to  $10\text{mm}$ ,  $w = 1\text{mm}$  to  $10\text{mm}$ , and  $L = 40\text{mm}$ . The results for  $d$  and  $w$  calculated to  $1\text{mm}$  were a maximum frequency of  $983\text{ Hz}$  in the open cavity and a minimum frequency of  $491\text{ Hz}$  in the closed cavity. Follows that a variety of frequency selections can be determined by  $L$ ,  $w$ , and  $d$  changes of the flange.

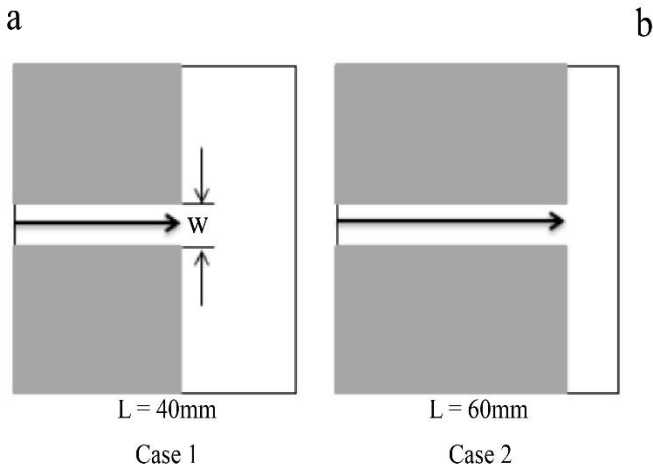


(c) Two different effective structures with closed cavities and varying length  $L$ , (d) Reflection coefficients inside the wavelength cavity for the two different effective mediums are shown in (c)

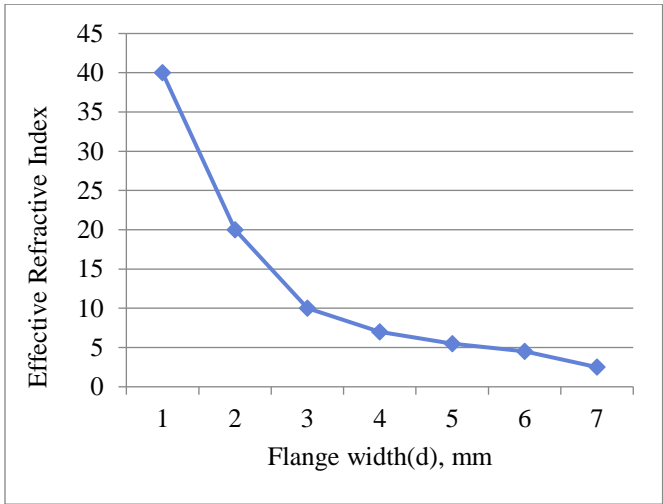
Fig. 2 Transmission and reflection coefficients in the effective medium



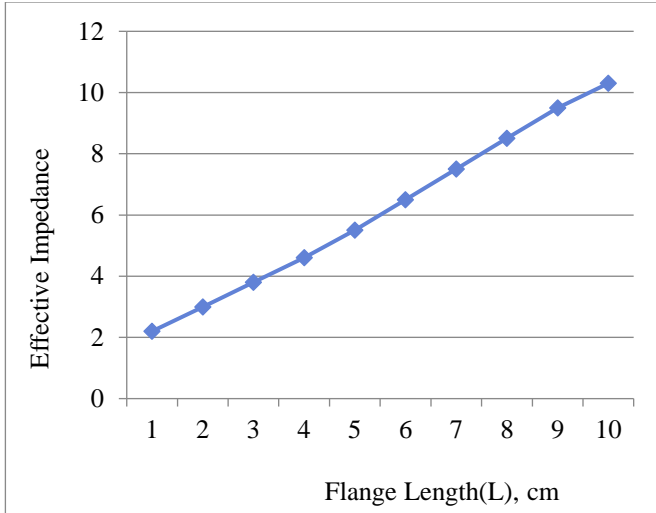
(a) The effective refractive index for open



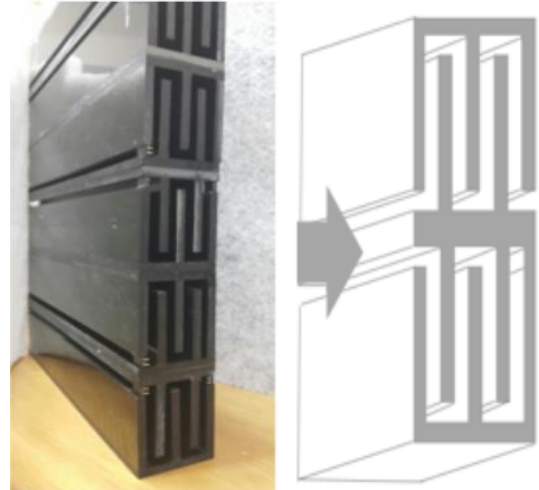
(a) Two different effective structures with open cavities and varying length  $L$ , (b) Transmission coefficients inside the wavelength cavity for the two different effective mediums are shown in (a)



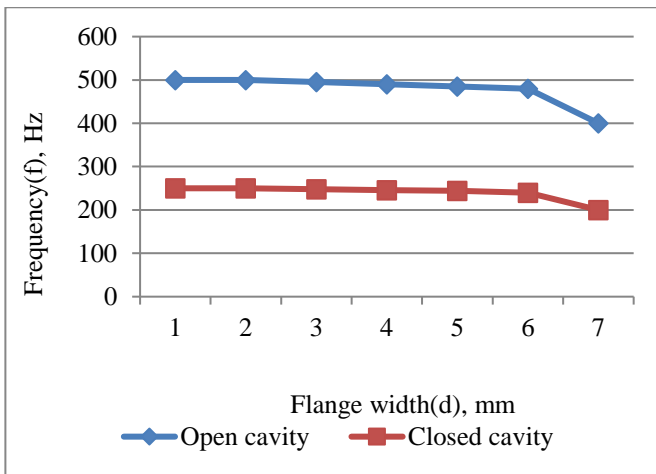
(b) Effective refractive index for closed



(c) Effective impedance of coiling up metamaterials for open

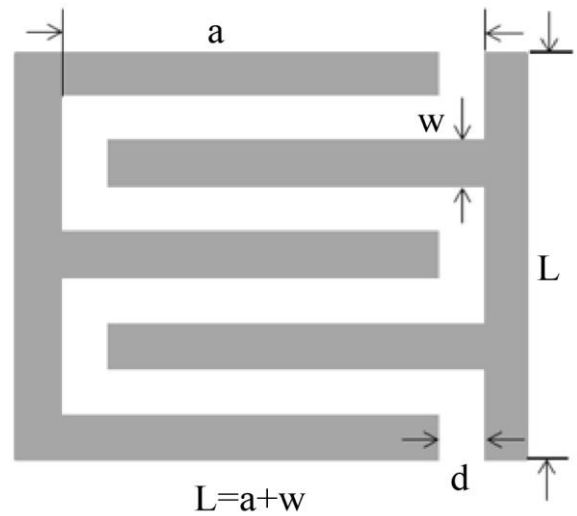


(a) The fabricated metamaterial samples consisting of an open cavity and a closed cavity



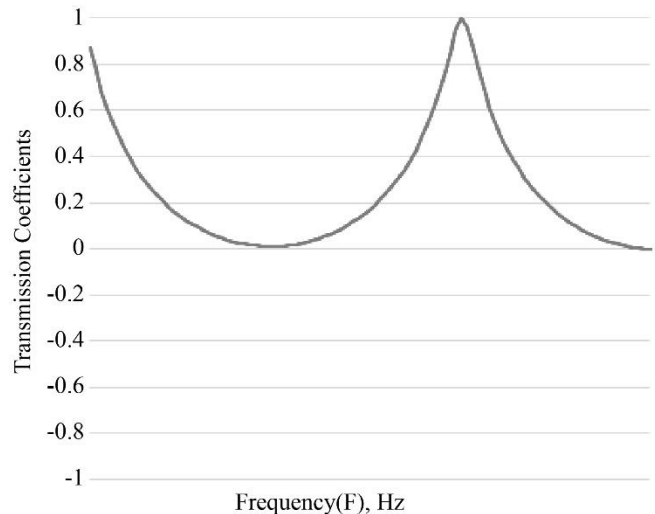
(d) Effective impedance of coiling up metamaterials for closed

Fig. 3 Effective refractive index and effective impedance of coiling up metamaterials

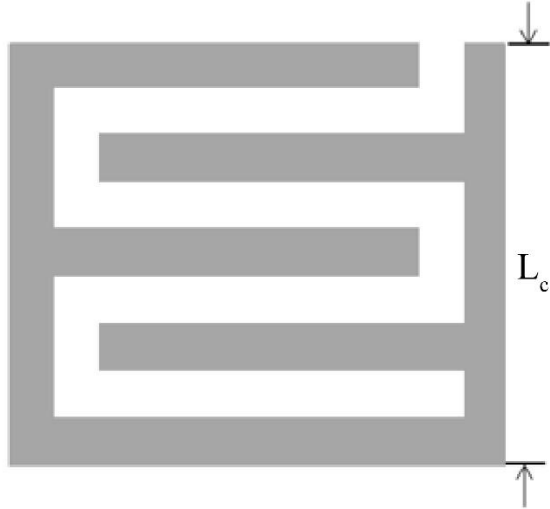


(b) The schematic of the unit cell with the  $w = 5\text{mm}$ ,  $d = 5\text{mm}$ ,  $a = 40\text{mm}$  for an open cavity

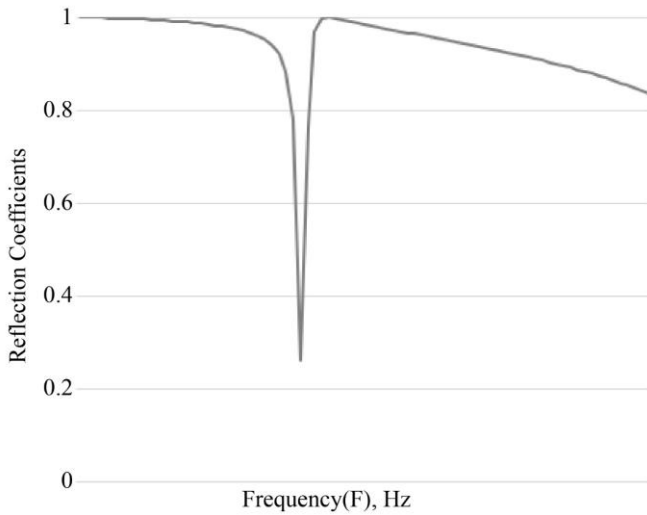
We designed a closed cavity and an open cavity for a coiling up structure with a unit cell size of  $L = 55\text{mm}$  (Figure 4 (a)). The elements inside the unit cell have the dimensions of  $a = 45\text{mm}$ ,  $w = 5\text{mm}$ ,  $d = 5\text{mm}$ . In order to obtain the theoretical frequency response and the sound pressure of the meta-material, we performed calculations with the software package COMSOL Multi-physics. In the normal direction, the incident wave on the slab was used for a plane wave. For our calculations, we used Young's modulus of  $8.5 \times 10^9 \text{ Pa}$ , a density of  $1011 \text{ kg/m}^3$ , and a Poisson's ratio of 0.33 to simulate the properties of aluminum and chose air as the fluid. For the open cavity, we analyzed the characteristics of the metamaterial, obtained the coefficients transmission (Figure 4 (b)), and the characteristics of the FP resonance appear periodically (Figure 4 (c)). For the closed cavity, we obtained the reflection coefficients (Figure 4 (d)), and this is confirmed by the reflected wave, which appears with resonant properties that match the coiling up structure (Figure 4 (e)) [2][9][10].



(c) The transmission coefficient of an open cavity with the unit cell



(d) The schematic of the unit cell with the  $w = 5\text{mm}$ ,  $d = 5\text{mm}$ ,  $a = 40\text{mm}$  for a closed cavity

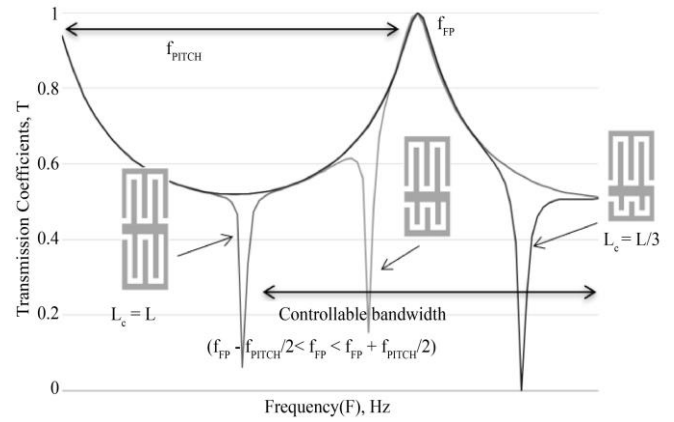


(e) The reflection coefficient of a closed cavity with the unit cell  
**Fig. 4 Design of two types of metamaterial cavities**

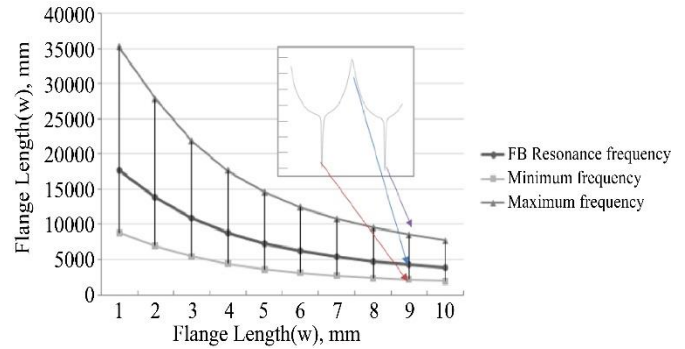
#### 4. Results and Discussion

Figure 5(a) shows the sound pressure for frequency response, which is calculated using three types of cavities in transmission parts. Here, the lengths  $L_c$  of the closed cavity with pressure reduction characteristics were 25mm, 30mm, 35mm and 45mm. Therefore, to decrease the desired frequency components, we can select a variety of frequencies according to the calculation formula. FP resonance frequency,  $f_{FP}$ , is determined for the open cavity in the calculation, and bandwidth of selectable stop-band frequencies with a dynamic range ( $f_{FP} - f_{PITCH}/2 < f_{FP} < f_{FP} + f_{PITCH}/2$ ) of the period,  $f_{PITCH}$  of the FP resonance frequency. The stop-band frequency range can be obtained by adjusting the unit cell of the closed cavity length, which is determined from the maximum FP resonance frequency. This experiment was performed to simulate COMSOL use of aluminum and air. The dimensions of the flange in the simulation are length ( $L$ )

45mm, width ( $w$ ) 5mm and depth ( $d$ ) 5mm. The open cavity used is a fixed size, and by adjusting the flange length  $L_c$  of the closed cavity, we can control a wide variety of locations of stop-band frequencies in the controllable bandwidth, BWc. Figure 5(b) shows how the dynamic frequency changes according to the length of the flange of the open cavity and the closed cavity. When the length of an open cavity,  $L$ , is 100mm, and the length of a closed cavity varies from 10mm to 100mm, the stop-band frequency can be adjusted from 380Hz to 770Hz.



(a) Comparison of the simulated data through two cavities of metamaterial according to the lengths ( $L_c$ ) of the closed cavity; the black lines represent the sound pressure of FP resonance in the open cavity, while the gray lines represent the calculated data in the closed cavity

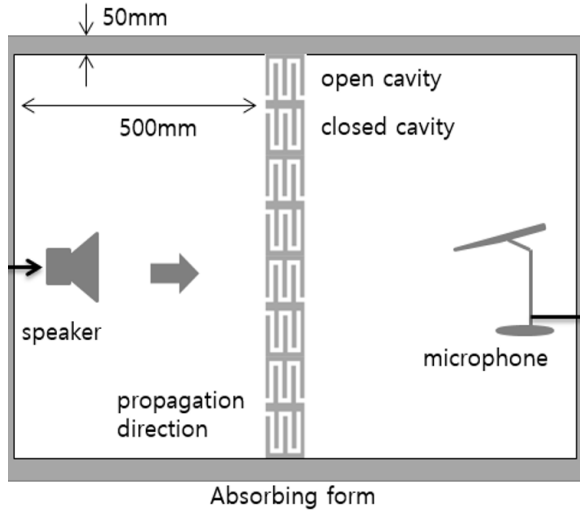


(b) Controllable bandwidth with the resonance of FP in the open cavity with fixed  $L$  and the stop-band resonance in the closed cavity according to the length of the flange ( $L_c$ ).

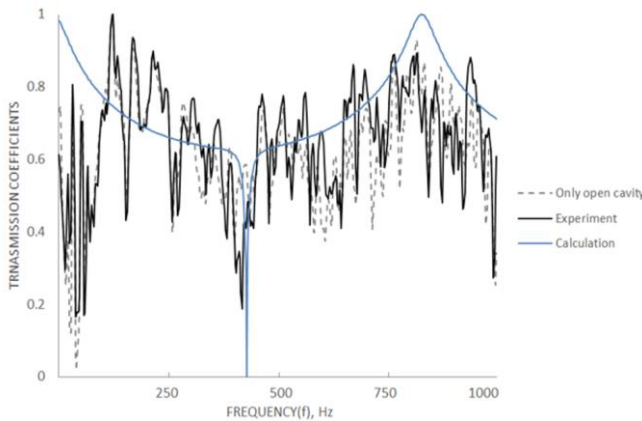
**Fig. 5 Control of sound pressure using our metamaterial**

The experimental method of this study was conducted with respect to the sound pressure analysis of the metamaterial. Sound pressure was calculated using COMSOL and a plane wave in the slab. In the experiment, sound pressure was measured using a white random signal. To evaluate the sound pressure, we used consist of two unit cells with coiling-up structures. The coiling-up structures consist of an open cavity and a closed cavity. In order to measure the sound pressure difference, the transmission coefficient and the reflection coefficient were measured and analyzed. In Figure 5(a), the calculated sound pressure and the measured sound pressure can be accurately matched. The controllable dynamic range is

from 400 Hz to 1,350 Hz, and the effective refractive index used was from 1.14( $L_c = 25\text{mm}$ ) to 2.23( $L_c = 45\text{mm}$ ). Figure 5(b) shows that the maximum frequency at FP resonance is 840 Hz, the minimum frequency at stop-band is 440 Hz, and the maximum frequency is 1350Hz.



(a) Experimental setup for measuring transmission



(b) Comparison of the experimental data of transmitted data through two cavities of metamaterial; the solid lines represent the experimental data, while the dashed lines represent the calculated data.  
 Fig. 6 Measurement of sound pressure

In order to verify our studies on acoustic wave propagation, the effect of our metamaterial structure theoretically and experimentally was investigated. In an absorbing form, the transmitted acoustic pressure was plotted in accordance with the direction of wave propagation for waves of various frequencies, as shown in Figure 6(a). The random signals used for measuring sound pressure were used at 100 Hz to 5,000 Hz. The length  $L$  of the metamaterial was 55 mm, and the material was made of aluminum. The chamber used for accurate measurements had dimensions of 1,000mm x 500mm x 500mm (Length x width x Height). The distance between the metamaterial and the speakers was 500 mm. To compare simulation and measurement, test measurements

were taken at a range of 400 Hz to 1,500 Hz. Figure 6(b) shows that the measured and calculated results are identical. In the flange, by changing the length of the closed cavity, this stop-band filter is performed at a range of frequencies from 440 Hz to 1,320 Hz.

In order to obtain the acoustic characteristics for this study, results in simulation were performed by using the simulation software package COMSOL Multi-physics. The calculation of sound pressure in various samples was carried out by consideration of the refractive index and the impedance in the cavity. The metamaterial samples in the experiment had a width ( $w$ ) of 10mm, a depth ( $d$ ) of 10mm and a length ( $L$ ) of 45mm and were designed and manufactured to the specification of 360mm x 500mm. We used a single-unit cell of two types with periodic boundary conditions for all the calculations. The sound amplitude in the metamaterial was measured by input from generating a white noise (100 Hz ~ 5,000 Hz) on the PC.

The acoustic signals of specified frequencies were generated using a virtual instrument via a commercial 5ohm speaker connected to the computer's soundcard. This speaker was powered to amplify the generated sound waves using a sound amplifier. Sound signals were acquired by a microphone connected to the soundcard. The SPL measurement in meta-material was carried to the sound pressure transmitted through the microphone and speaker in the absorbing form, and the distance between the metamaterial and the speaker was 1,000mm. In order to compare the calculated and experimental evaluation of the results, the measurement frequency for the sound pressure in metamaterial is used a bandwidth of 440Hz to 1,350 Hz. In order to compare the relative evaluation, the amplitude of sound pressure was compared using the transfer function of the reference SPL and cavity SPL.

## 5. Conclusion

In this study, we design a metamaterial that attenuates desired frequency components using open and closed coiling structures. In particular, we confirmed that it performs better in the part that emphasizes or reduces low-frequency characteristics in the experiment, so we focused on the frequencies between 400 Hz and 1500 Hz. In the structure and sound concentration space used in the experiment, we can emphasize diversity with excellent spatial changes rather than the specificity shown in existing structures.

There has been no research on structures that provide various changes to specific frequencies yet, and we obtained the advantage of being applicable to various structures and verified it through experiments. We obtained successful results by comparing theoretical calculations and experimental measurements. The results were designed to be suitable for small scales to be applied to highly effective refractive indices. The metamaterial based on the FP

resonance theory was calculated as an effective coefficient for analyzing the characteristics of open and closed cavities. Both open and closed structures can overcome the shortcomings shown in existing studies and can be changed into various structures.

The metamaterial, using a combination of the characteristics of the two cavities, appropriately maintained the FP resonance and performed a band-stop filter function. This study is advantageous in changing the acoustic characteristics by designing the cavity and other spaces separately. It especially affects the change of low-frequency components rather than high-frequency components. For this reason, we show a method to design an acoustic filter by changing the length and width. We propose a metamaterial design based on transmission and reflection at FP resonance.

The experimental and numerical results are in good agreement, and it is experimentally shown that it maintains FP resonance and removes redundant frequencies in amplitude. In the future, this study can be applied more widely to acoustic applications using existing acoustic metamaterials by reflecting the characteristics of various structures, and it is expected to play an important role in the field of basic metamaterials. In particular, it can be applied in various ways by applying the characteristics to special structures rather than applying them to monotonous structures. The results presented and tested in this paper can be potentially applied to acoustic filtering, absorption, and imaging.

### Acknowledgements

This Research was supported by Kangnam University Research Grants (2023).

### References

- [1] Lucian Zigoneanu, Bogdan-Ioan Popa, and Steven A. Cummer, "Three-Dimensional Broadband Omnidirectional Acoustic Ground Cloak," *Nature Materials*, vol. 13, no. 4, pp. 352-355, 2014. [[CrossRef](#)] [[Google Scholar](#)] [[Publisher Link](#)]
- [2] Kyungjun Song et al., "Sound Pressure Level Gain in an Acoustic Metamaterial Cavity," *Scientific Reports*, vol. 4, no. 1, 2014. [[CrossRef](#)] [[Google Scholar](#)] [[Publisher Link](#)]
- [3] Xiaoshi Su, and N. Andrew Norris, "Focusing, Refraction, and Asymmetric Transmission of Elastic Waves in Solid Metamaterials with Aligned Parallel Gaps," *Journal of the Acoustical Society of America*, vol. 139, no. 6, pp. 3386-3394, 2016. [[CrossRef](#)] [[Google Scholar](#)] [[Publisher Link](#)]
- [4] Andrea Colombi, Philippe Roux, and Matthieu Rupin, "Sub-Wavelength Energy Trapping of Elastic Waves in a Metamaterial," *Journal of the Acoustical Society of America*, vol. 136, no. 2, pp. 192-198, 2014. [[CrossRef](#)] [[Google Scholar](#)] [[Publisher Link](#)]
- [5] Bogdan-Ioan Popa, and A. Steven Cummer, "Non-Reciprocal and Highly Nonlinear Active Acoustic Metamaterials," *Nature Communications*, vol. 5, no. 1, pp. 1-5, 2014. [[CrossRef](#)] [[Google Scholar](#)] [[Publisher Link](#)]
- [6] Juliette Pierre, Benjamin Dollet, and Valentin Leroy, "Resonant Acoustic Propagation and Negative Density in Liquid Foams," *Physical Review Letters*, vol. 112, no. 14, 2014. [[CrossRef](#)] [[Google Scholar](#)] [[Publisher Link](#)]
- [7] Kyungjun Song et al., "Emission Enhancement of Sound Emitters using an Acoustic Metamaterial Cavity," *Scientific Reports*, vol. 4, no. 1, pp. 1-6, 2014. [[CrossRef](#)] [[Google Scholar](#)] [[Publisher Link](#)]
- [8] Zixian Liang et al., "Space-Coiling Metamaterials with Double Negativity and Conical Dispersion," *Scientific Reports*, vol. 3, no. 1, pp. 1-6, 2013. [[CrossRef](#)] [[Google Scholar](#)] [[Publisher Link](#)]
- [9] Romain Fleury, and Andrea Alù, "Extraordinary Sound Transmission through Density-Near-Zero Ultranarrow Channels," *Physical Review Letters*, vol. 111, no. 5, 2013. [[CrossRef](#)] [[Google Scholar](#)] [[Publisher Link](#)]
- [10] Yong Li et al., "Unidirectional Acoustic Transmission Through a Prism with Near-Zero Refractive Index," *Applied Physics Letters*, vol. 103, no. 5, 2013. [[CrossRef](#)] [[Google Scholar](#)] [[Publisher Link](#)]
- [11] Jie Zhu et al., "Acoustic Rainbow Trapping," *Scientific Reports*, vol. 3, no. 1, pp. 1-6, 2013. [[CrossRef](#)] [[Google Scholar](#)] [[Publisher Link](#)]